Inhibition of alkaline corrosion of mild Steel using synthetic 2-(4-Methylphenylsulphonamido)-3-methylbutanoic acid.

Abstract

Aim: To study the corrosion inhibition performance of 2-(4-Methylphenylsulphonamido)-3-methylbutanoic acid (MPSMB) on mild steel in 0.1 M KOH.

Study design: The study will investigate the inhibitive performance of the inhibitor at different concentrations and immersion times as well as test its electrochemical corrosion properties. Theoretical simulation will be used to correlate the experimental results.

Place and duration: Imo state University Owerri, Imo State Nigeria. Between June 2022 and May 2023

Methodology: Gravimetric, electrochemical and simulation methods.

Results: The obtained gravimetric results showed that the inhibitor reduced mild steel corrosion in the studied environment and that the efficacy of the inhibitor improved with increased concentration of the inhibitor. Polarization findings revealed that the inhibitor retarded the corrosion reactions in a mixed-mode manner while electrochemical impedance spectroscopy and theoretical simulation findings were used to complement the obtained results.

Conclusion; the results obtained showed that 2-(4-Methylphenylsulphonamido)-3-methylbutanoic acid effectively retarded the corrosion of mild steel in 0.1 M KOH.

Keywords: corrosion, 2-(4-Methylphenylsulphonamido)-3-methylbutanoic acid, electrochemistry, impedance, Density functional theory

1. Introduction

Corrosion of mild steel is one of the major industrial problems encountered in modern societies. One of the most effective ways of combating this menace is the use of corrosion inhibitors, these are chemicals that efficiently slow the rate of corrosion of metals and alloys when used in low concentrations, especially in cooling systems, boilers and storage vessels oil as well as gas pipelines, and in construction industries (1-3). Mild steel (MS) is leading construction material as a result of its outstanding mechanical properties and low costs when compared to other materials, however being a metallic alloy, it is susceptible to corrosive degradation. This operation needs to be check especially in the presence of extremely damaging corrosive alkaline solutions. Mild steel corrosion in alkaline solution has been effectively reduced by the use of synthetic organic substances containing oxygen, nitrogen, or sulphur in the

conjugated system as corrosion inhibitors (4-8). The adsorption of these inhibitors on the metal / solution interface is successively influenced by: (i) nature and charge on the metal surface; (ii) type of corrosive electrolyte; and (iii) molecular structure of corrosion inhibitors (9-10) Successful use of naturally occurring materials in both acidic and alkaline environments has been extensively reported (11-16). Computer simulation techniques provides understanding of inhibition adsorption properties of inhibitors at the molecular level thereby supporting the experimental results during the corrosion control using inhibitors. Among the computer simulation methods, density functional theory (DFT) is a valid tool in evaluating corrosion inhibitive properties of different materials [17–19]. This work reports the inhibition of alkaline corrosion of mild steel in the presence of 2-(4-Methylphenylsulphonamido)-3-methylbutanoic acid. The techniques applied are gravimetric, electrochemistry and theoretical simulation using DFT.

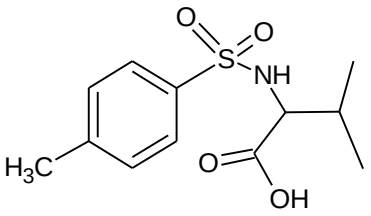

2 -(4-Methylphenylsulphonamido -3-methylbutanoic acid

Figure 1. Chemical structure of the inhibitor

2. Materials and methods

2.1 Preparation of Inhibitor

The 2-(4-Methylphenylsulphonamido)-3-methylbutanoic acid used for the corrosion inhibition reactions was synthesized in the organic chemistry laboratory of the Imo State University, Owerri (20). 5 g of the inhibitor was dissolved in 1 liter of 96 % pure ethanol to give a stock solution of concentration 5g/L. Test solutions (0.2 g/L, 0.3 g/L & 0.4 g/L) were prepared from the stock solution in 0.1 M KOH.

2.2 **Preparation of mild steel specimen**

The metal steel specimens used for the corrosion tests have the percentage weight composition: C-0.05, Mn-0.6, P-0.36, Si-0.3 and Fe-98.69 [21], the mild steel was obtained from a commercial source in Imo State and then press cut into dimensions of 3 x 3 x 0.14 cm for the gravimetric experiments and 1 cm x 1 cm x 0.14 cm. for the electrochemical experiments and kept in a moisture free desiccator for use when needed.

2.2 Gravimetric experiments

Gravimetric tests were conducted on mild steel coupons of dimension 3 cm x 3cm x 0.14 cm. the metal coupons were polished while wet with silicon carbide abrasive paper from #100 to1000 (22), washed under running water, degreased in acetone and dried with warm air. The gravimetric work station was set up by suspending the metal coupons with hook and rod in 300 ml of the test solution. The experiments were conducted in aerated and unstirred solutions.

2.3 Electrochemistry experiments

All the electrochemical experiments were conducted in a 3-electrode corrosion cell using a VERSASTAT 400 Complete DC Voltammetry and Corrosion System with V3 studio software. A graphite rod was used as the counter electrode while a saturated calomel electrode (SCE) was used as reference electrode. The latter was connected using a Luggins capillary. The experiments were conducted in aerated and unstirred solutions at the end of 1 hour immersion time at 303 K. The electrochemical impedance spectroscopy (EIS) measurements were conducted at corrosion potentials (E_{corr}) over a frequency range of 100 kHz–10 mHz, the signal amplitude perturbation was 5 mV. Potentiodynamic polarization (PDP) studies were conducted in the potential range ±250 mV versus corrosion potential at a scan rate of 0.333 mV/s. Each test was run in triplicate to ensure good reproducibility of the obtained data.

2.4 Theoretical Simulations

All the theoretical calculations were done using the density functional theory (DFT) electronic structure programs Forcite and DMol3 as contained in the Materials Studio 4.0 software (Accelrys, Inc.)

3. Results

3.1 Gravimetric Results

The inhibitive performance of MPSMB on the corrosion of mild steel in 0.1 M KOH was investigated using the gravimetric corrosion monitoring technique, the results are presented in figures 2 and 3. The results presented are averages of triplicate determinations, and standard deviation ranges from 0 to 0.0006. Figure 2 shows the average weight loss of mild steel in uninhibited and inhibited 0.1 M KOH as a function of inhibitor concentration. The results indicate that the synthetic MPSMB significantly reduced the degradation rates in the alkaline environment. The result shows that average weight loss reduced with increasing inhibitor concentration. Figure 3 shows the relationship between the percentage inhibition efficiency and inhibitor concentration for mild steel corrosion in 0.1 M KOH and it shows that the efficacy of the inhibitor increased with concentration.

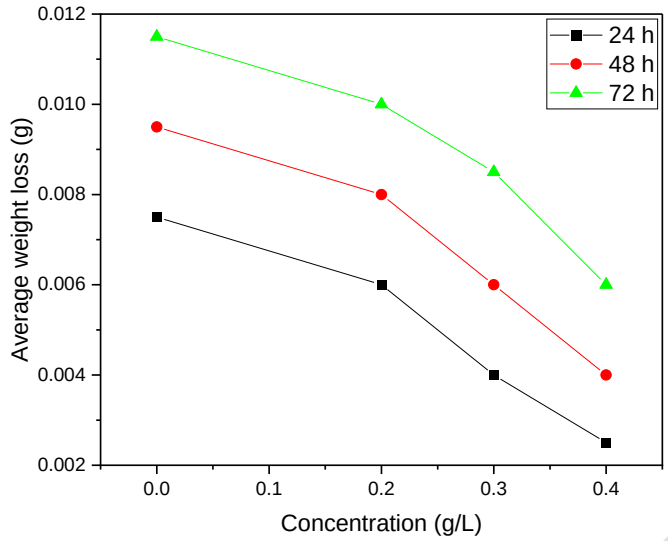

Figure 2. Average weight losses of mild steel in 0.1 M KOH solutions without and with PMPSP extract, as a function of inhibitor concentration.

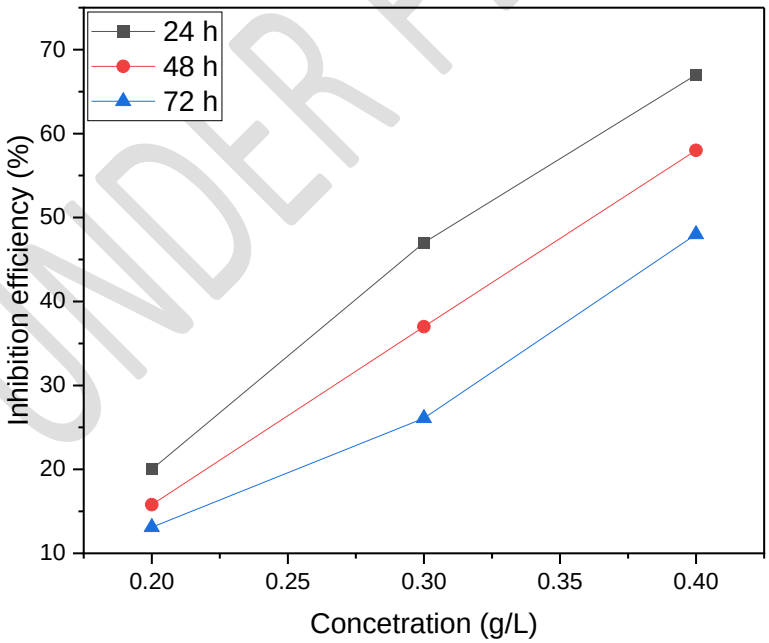

Figure 3. Relationship between percentage inhibition efficiency of PMBSP and concentration for mild steel corrosion in 0. 1 M KOH solutions**.**

The corrosion inhibition efficiency of MPSMB on mild steel corrosion was quantified from the gravimetric perspective as follows:

$$IE\ (\%) = \left(1 - \frac{\Delta W_{inh}}{\Delta W_{bl}}\right) \times 100 \quad (1)$$

Where ΔW_{inh} and ΔW_{bl} correspond to the weight losses with and without the inhibitor solution respectively.

3.2 Electrochemistry Results

(a) Electrochemical impedance spectroscopy (EIS) results

The impedance data provides information on the kinetics of the electrochemical reactions and also provides insight into the corrosion mechanism at the Fe/0.1 M KOH interfaces in absence and presence of the PMBSP inhibitor. The impedances response in the Nyqiust format is shown in Figures 4 for mild steel corrosion without and with the inhibitor while Table 1 shows the electrochemical data obtained from the electrochemical experiments. The impedance plots can be seen to be composed of one depressed capacitive half circle in a high-frequency region. The depression seen in the Nyquist half circle with center under the real axis is a characteristic of solid metal electrodes which show frequency dispersion of the impedance response. It is worthy to note that the high-frequency intercept with the real axis seen in the Nyquist semicircle is allocated to the solution resistance (Rs), also the low-frequency intercept with the real axis is assigned to the charge transfer resistance (Rct). The EIS data was fitted into an equivalent circuit $\mathrm{R_s}\left(\mathrm{Q_{dl}R_{ct}}\right)$ (23) which has been previously used to fit impedance data. The solution resistance is shorted by a constant phase element (CPE) in the equivalent circuit, lying parallel to the charge transfer resistance (R_{ct}). The use of the CPE in place of capacitor is to compensate for shift from ideal dielectric characteristic arising from the use of heterogeneous electrode surfaces

The impedance of the CPE element is given as below:

$$Z_{CPE} = Q^{-1}(j\omega)^{-n} \quad (2)$$

Where Q and n respectively represents CPE constant and exponent,
j is an imaginary number which is $= (-1)^{1/2}$, and ω stands for the angular frequency in $rad\ s^{-1}$ with value $2\pi f$ and f is the frequency in Hz. The result in Table 1 show that the inhibitor increased the value of the charge transfer resistance (R_{ct}) and this corresponds to the increase in the semicircle diameter in the Nyquist plot. This effect confirms that the inhibitor actually retarded the corrosion of mild steel in the alkaline environment. The inhibition efficiency tabulated in Table 1 was obtained from the impedance data with the formula below:

$$IE\ (\%) = \frac{R_{ct\ inh} - R_{ct\ bl}}{R_{ct\ inh}} \times 100 \qquad (3)$$

Where $R_{ct\ bl}$ is the charge transfer resistance in the absence of the inhibitor and $R_{ct\ inh}$ is the charge transfer resistance in the presence of the inhibitor. The values of the inhibition efficiencies obtained in Table 1 agree significantly with those obtained in the gravimetric experiments.

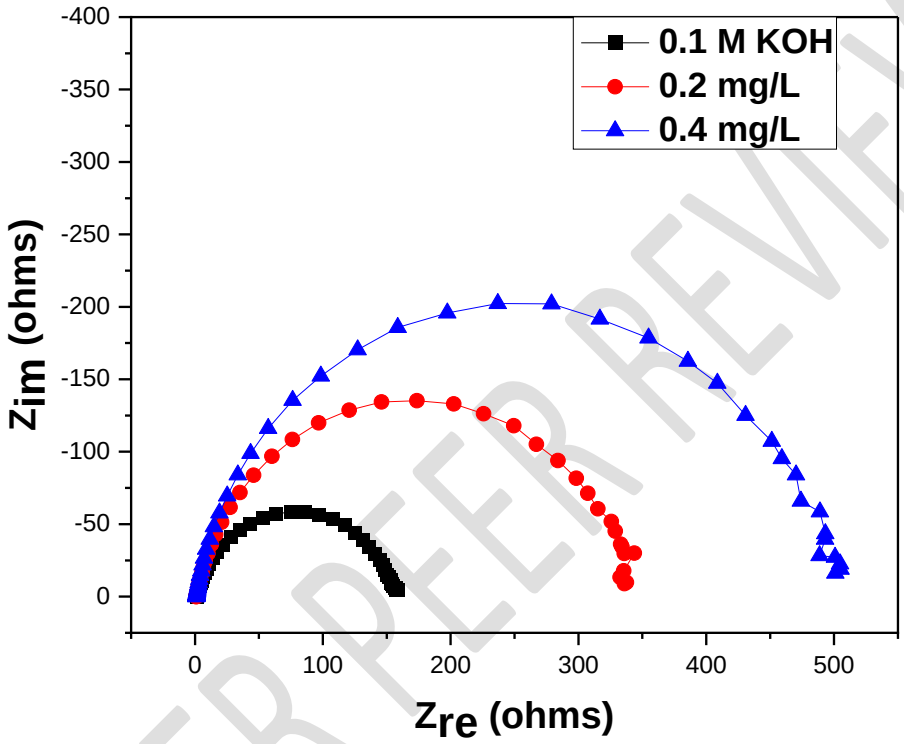

Figure 4. Electrochemical impedance spectroscopy for Mild steel in 0.1 M KOH in the absence and presence of the inhibitor.

(a) Potentiodynamic polarization (PDP)results

To ascertain the effect of the inhibitor on both the anodic dissolution of mild steel and cathodic evolution of hydrogen, potentiodynamic polarization experiments were undertaken. Typical potentiodynamic polarization plots for the corrosion of mild steel in the absence and presence of the inhibitor are presented in Figure 5 while the polarization parameters are presented in Table 1. increase in the concentration of the inhibitor can be seen to have affected both the cathodic as well as the anodic half reactions shifting the corrosion potential (E_{corr}) slightly towards the more negative values as well as reducing the anodic and cathodic current densities and also the corrosion current density (E_{corr}) showing that the inhibitor is a mixed type

corrosion inhibitor for mild steel in alkaline solution. The inhibition efficiencies from the PDP data was obtained by comparing the corrosion current densities in uninhibited ($i_{corr\ bl}$) solution with that from the inhibited solution ($i_{corr\ inh}$) as below:

$$\%IE = \frac{i_{corr\ bl} - i_{corr\ inh}}{i_{corr\ bl}} \times 100 \quad (4)$$

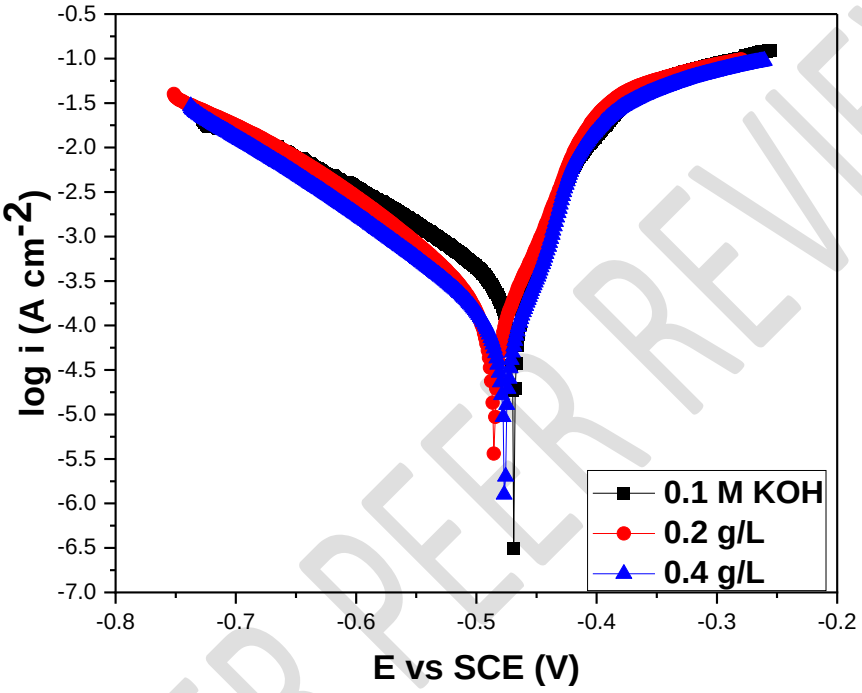

Figure 5: Potentiodynamic polarization curves of Mild steel in 0.1 M KOH in the absence and presence of the inhibitor.

Table 1. Electrochemical Parameters for Mild steel in 0.1 M KOH in the Absence and Presence of the inhibitor.

System	E_{corr} (mV vs SCE)	I_{corr} (μA/cm^2)	IE%	R_{ct} (Ωcm^2)	n	I.E%
0.1 M KOH	**- 463**	**210.3**		**155.2**	**0.88**	

0.2 g/L	- 483	69.7	66.9	349.7	0.88	55.6
0.4 g/L	- 494	40.3	80.8	494.6	0.89	68.6

3.3 Theoretical Results

Density functional theory and molecular dynamic simulation calculations which have been used previously to correlate experimental and computational results (24-25) were undertaken to ascertain the corrosion inhibiting behavior of the PMBSP from the theoretical point of view. In the recent era of software advancement, corrosion experts normally choose an inhibitor on the basis of the theoretical analysis of its molecular properties; this approach is both cheap as well as effective when compared to the experimental approach. Density functional theory (DFT) was used to calculate information relating molecular geometries and electron distributions of the inhibitor, which influence corrosion inhibition reaction. DFT calculations were done using electronic structure DMol3 found in a Mulliken population analysis. The Electronic parameters used in this simulation were the Perdew−Wang (PW) local correlation density functional as well as the restricted spin polarization by using the DND basis set. For core electrons at the lowest atomic orbitals the DFT semicore pseudopotentials (DSPP) was used.

Geometric optimization was achieved using COMPASS force field (26) as well as Smart minimization methods, in order to predict the activity of the inhibitor towards the metal surface, the quantum chemical parameters such as the lowest unoccupied molecular orbital (E_{LUMO}), the highest occupied molecular orbital energy (E_{HOMO}) and energy gap (ΔE) were calculated and their values are respectively E_{LUMO} =-2.181eV , E_{HOMO} =-6.041eV and ΔE=3.86. The representative snapshots of the optimized structure of the inhibitor, LUMO orbital, HOMO orbitals, and the total electron density are presented in Figure 6 as estimated from the simulations.

Forcite quench molecular dynamics was used to simulate different low energy adsorption configurations of the inhibitor molecule on the metal surface (27-28). The metal (Fe) crystal was cleaved along an (110) plane because it was the most density packed Fe surface and stable (29-30). Calculations were done in a supercell of dimension 12x10 using the smart algorithm with NVE (microanonical) and the COMPASS force field in a simulation box of dimension 30 A˚ x 9 25 A˚ x 9 29 A˚ with periodic boundary conditions to model a representative part of the interface, devoid of arbitrary boundary effects. The box contained the metal slab; cleaved along the Fe(110) plane and a vacuum layer of height 20 A˚. The step time was 1 fs and the simulation time was 5 ps. The temperature was set at 350 K and the geometry of the lower layers of the slab was constrained. The optimized structure of the inhibitor was used for the simulation. Quenching was done at every 250 steps. The representative snap shot of the optimized structure of the inhibitor in the 12x10 supercell is shown in Figure 7. The Binding energy which relates the adsorption of the inhibitor to its inhibition efficiency was estimated with the equation below:

$$E_{bind} = E_{total-}\left(E_{inhibitor} + E_{metal\ surface}\right) \quad (5)$$

Where E_{total}, $E_{inhibitor}$ and $E_{metal\ surface}$, represent the energy of the system containing both the metal surface and the inhibitor, the energy of the single inhibitor molecule and the energy of the metal surface without the inhibitor respectively. The negative value of adsorption energy **(-133.17)** indicates strong adsorption of the inhibitor on the metal surface and points to good corrosion inhibiting property.

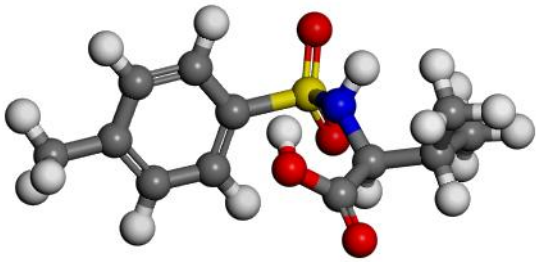

Optimized Structure

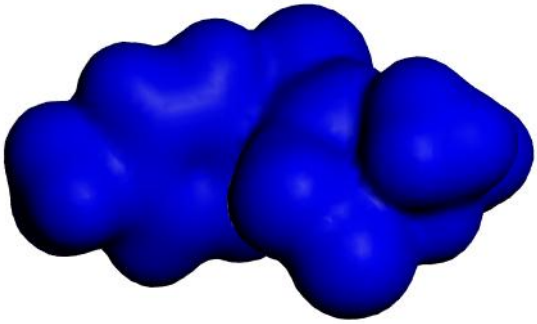

Electron density

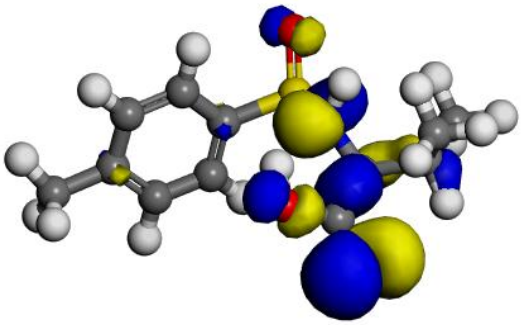

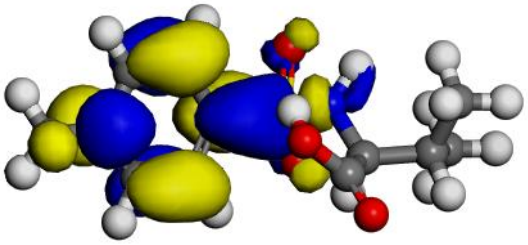

HOMO **LUMO**

Figure 6. Electronic properties of 2-(4-Methylphenylsulphonamido)-3-methylbutanoic acid. (atom legend: white H, light gray C and dark gray O). The isosurfaces (larger lobes) depict the electron density difference; the darker regions show electron accumulation, whereas the lighter regions show electron loss

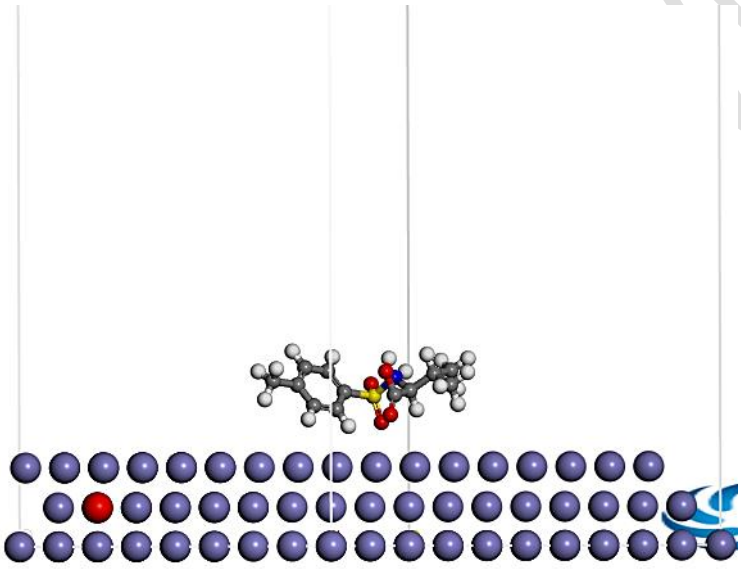

Figure 7. Representative snapshots of 2-(4-Methylphenylsulphonamido)-3-methylbutanoic acid on the metal surface.

Conclusion

The mild steel corrosion inhibition properties of 2-(4-Methylphenylsulphonamido)-3-methylbutanoic acid was investigated in 1 M KOH solution using gravimetric, electrochemistry and theoretical methods of monitoring corrosion. The gravimetric results showed that the inhibitor lowered the corrosion of mild steel in the studied environment and that inhibition efficiency increased with the concentration of the inhibitor and reduced gradually with time. The electrochemistry results showed that both the anodic and cathodic corrosion reactions were reduced with the addition of the inhibitor which implied that the inhibitor functioned as a mixed type corrosion inhibitor for mild steel in the alkaline environment. The simulation result showed a negative adsorption energy which is an indication of a good corrosion inhibitor.

References

1. Al-Amiery A. A, Mohamad A, Kadhum A. H. , Shaker L.M , Isahak W N, Takrif M S. Experimental and theoretical study on the corrosion inhibition of mild steel by nonanedioic acid derivative in hydrochloric acid solution, Scientific Report, 2022: (12):4705, doi.org/10.1038/s41598-022-08146-8.
2. Timothy, M. N, Iyama, W. A, Maduelosi, N. J Assessment of the corrosion inhibition potentials of terminalia ivorensis leaves extract on steel in alkali medium. journal of applied chemical science international, 2019 :10 (1): 36–44.
3. Garai S Garai S Jaisankar P Singh J K. Elango, A. A comprehensive study on crude methanolic extract of Artemisia pallens (Asteraceae) and its active component as efective corrosion inhibitors of mild steel in acid solution. Corrosion Science 2012: (60) 193–204.
4. Ambrish, S V Singh K Quaraishi M A. Aqueous Extracts of Kalmegh (Andrographis paniculata) leaves as green inhibitors for mild steel in Hydrochloric acid solution 2010 International Journal of Corrosion. Article ID: 275983. .1-11
5. Axelrod G S. A process for the preparation of natural salt formulations for seawater substitution, mineral fortification. Publication no 2005 WO2013098857 A1, 1-3
6. Raja, P. B. et al. Evaluation of green corrosion inhibition by alkaloid extracts of Ochrosia oppositifolia and Isoreserpiline against mild steel in 1 M HCl medium. Ind. Eng. Chem. Res 2013 :52 10582–10593.
7. Bammou L, Belkhaouda. M R. Salghi O. Benali A. Zarrouk H. Zarrok , B. Hammouti. Corrosion inhibition of steel in sulfuric acidic solution by the Chenopodium Ambrosioides Extracts 2013 Journal of the Association of Arab Universities for Basic and Applied Sciences ; 16: 83–90
8. James A O. Okafor N C. Abiola O. K Inhibition of Acid Corrosion of Mild Steel by Pyridoxol hydrochlorides 2007 International Journal of Electrochemical Science, Serbia, 1: 80–91.
9. Ahamad I. Quraishi M. A. Bis (benzimidazol-2-yl) disulphide: An efficient water soluble inhibitor for corrosion of mild steel in acid media 2009 Corrosion Science 51, 2006-2013
10. Al-Dokheily M A. Kredy H M. Al-Jabery R. N. Inhibition of Copper Corrosion in H2SO4, NaCl and NaOH Solutions by Citrullus colocynthis Fruits Extract 2014 Journal of Natural Sciences Research .4: (17)
11. Jiang, W Gong M Zhao J Progress of research on green corrosion inhibitors extracted from natural plants 2017, Corrosion Science and protection Technology, China 9 :(4): 0278.
12. Abiola O K. Oforka N.C, Inhibition of the Corrosion of Mild Steel in Hydrochloric Acid by (4- Amino – 2 –Methyl-5-Pyrimidinyl Methylthio) Acetic Acid and its Precursor 2002 Journal of Corrosion Science and Engineering :3: 1-8.
13. El Bribri, A., Tabyaoui, M., Tabyaoui, B., El Attari, H. Bentiss, F. The use of Euphorbia falcata extract as eco-friendly corrosion inhibitor of carbon steel in hydrochloric acid solution 2013 Mater. Chem. Phys. :141: 240–247.
14. Behpour, M., Ghoreishi, S. M., Khayatkashani, M. Soltani, N. Green approach to corrosion inhibition of mild steel in two acidic solutions by the extract of Punica granatum peel and main constituents. 2012 Mater. Chem. Phys. 131, 621–633.
15. Pereira, S. S. A. A. et al. Inhibitory action of aqueous garlic peel extract on the corrosion of carbon steel in HCl solution. 2012 Corrosion Science :65: 360–366.

16. Uwah, I. E., Okafor, P. C. Ebiekpe, V. E. Inhibitive action of ethanol extracts from Nauclea latifolia on the corrosion of mild steel in H_2SO_4 solutions and their adsorption characteristics 2013 Arabian Journal Chemistry: 6: 285–293.
17. Cruz J, Pandiyan T, Garcia-Ochoa E. A new inhibitor for mild carbon steel: electrochemical and DFT studies 2005 Journal of Electroanal Chemistry 583:8–16
18. Khaled K F Corrosion control of copper in nitric acid solutions using some amino acids—a combined experimental and theoretical study. 2010 Corrosion Science 52:3225–3234
19. Oguzie E E, Akalezi C O, Enenebeaku C K, Aneke J N Corrosion inhibition and adsorption behavior of malachite green dye on aluminum corrosion. 2011 Chemical Engineering Commununication 198:46–60
20. Ikpa C B.C Okoro U C, Synthesis of New Paratoluene Sulphonamide Derivatives of Amino Acids And Their Anti Bacterial Activities, 2016 IOSR Journal Of Applied Chemistry (IOSR-JAC), 9 (6): 31-34.
21. Adindu B. Ogukwe C Eze F. Oguzie E, Exploiting the Anticorrosion Effects of Vernonia Amygdalina Extract for Protection of Mild Steel in Acidic Environments, 2016 Journal of Electrochemical Science and Technology, 7:(4): 251-262.
22. Alinanuswe J. M. Corrosion Inhibition of Mild Steel in Sulphuric Acid Solution with Tetradenia riparia Leaves Aqueous Extract: Kinetics and Thermodynamics, 2023 Biointerface research in applied Chemistry, 13: (1) 32 https://doi.org/10.33263/BRIAC131.032.
23. Oguzie E E Adindu C B Enenebeaku C K Ogukwe C E Chidiebere M A Oguzie K L. Natural Products for Materials Protection: Mechanism of Corrosion Inhibition of Mild Steel by Acid Extracts of Piper guineense, 2012ACS journal of physical chemistry, dx.doi.org/10.1021/jp300791s | J. Phys. Chem. C :116: 13603−13615.
24. Singh, M. R., Gupta, P. & Gupta, K. Te litchi (Litchi Chinensis) peels extract as a potential green inhibitor in prevention of corrosion of mild steel in 0.5 M H_2SO_4 solution 2015 https://doi.org/10.1016/j.arabjc.2015.01.002.
25. . Znini, M. et al. Essential oil of Salvia aucheri mesatlantica, as a green inhibitor for the corrosion of steel in 0.5M H2SO4. 2012. Arabian Journal of Chemistry (5) 467–474 .
26. Bello A U , Adamu U. Gideon A. Understanding Inhibition of Steel Corrosion by Some Potent Triazole Derivatives of Pyrimidine through Density Functional Theory and Molecular Dynamics Simulation Studies, 2019 Journal of the Turkish chemical society, . JOTCSA. ; 6(3): 451-462.
27. Casewit, C. J.; Colwell, K. S.; Rappe, A. K. Application of universal force field to main group elements 1992 Journal of American Chemical Society 114, 10046−10053.
28. Obot, I. B.; Obi-Egbedi, N. O.; Eseola, A. O. Anticorrosion potential of 2-mesityl-1H-imidazo[4,5-f][1,10]-phenanthroline on mild steel in sulfuric acid solution: Experimental and theoretical study 2011 Ind. Engineering Chemical Research 50, 2098−2110.
29. Bereket G, Öğretir C, Özşahin Ç. Quantum chemical studies on the inhibition efficiencies of some piperazine derivatives for the corrosion of steel in acidic medium. Journal of Molecular Structure 2003 THEOCHEM. ;663(1-3):39-46.
30. Nwankwo H U, Olasunkanmi L O, Ebenso E E. Experimental, quantum chemical and molecular dynamic simulations studies on the corrosion inhibition of mild steel by some carbazole derivatives. 2017 Scientific reports. ;7(1):2436.